A Comparison of Uncertainty Evaluation Methods for On-Wafer S-Parameter Measurements

A Comparison of Uncertainty Evaluation Methods for On-Wafer *S*-Parameter Measurements

Valeria Teppati, *Senior Member, IEEE*, and Andrea Ferrero, *Fellow, IEEE*

***Abstract*— An experimental analysis of on-wafer *S*-parameter uncertainties is presented. Recently, two different approaches, based either on differential numerical programming or on a fully analytical solution, have been introduced. In order to establish their suitability, a careful comparison is given for on-wafer measurements. Through this comparison, possible limitations and causes of errors are also highlighted. Finally, the uncertainty evaluation of the 16-term error model is presented for the first time.**

***Index Terms*— Calibration, measurement techniques, measurement uncertainty, millimeter wave devices, millimeter wave technology.**

I. Introduction

THE TREATMENT of uncertainties in *S*-parameter measurements is a topic of long-standing interest. Several issues remain open or under continuous development, e.g., the improvement of coaxial or waveguide interfaces and their repeatability [1], [2], or the traceability of the calibration standards to physical dimension measurements [3]–[5]. This is especially true as the frequency increases [6].

In a general case, *S*-parameter uncertainty evaluation is a fairly complex statistical problem, since the final result is a function of measurement noise, connection repeatability, and standard uncertainty. As is well known from experience, these contributions weigh differently on the device under test (DUT) uncertainty, depending on the chosen calibration algorithm.

Modern measurement software play a fundamental role in the overall measurement capabilities, and until the introduction of the two software tools here examined, a general approach for uncertainty evaluation was not available. This calls for a careful scientific evaluation of the performances of the two applications. In fact, the reported solutions are limited to specific calibration algorithms [7]–[11] or use time-consuming Monte Carlo methods [12]–[15]. Other techniques are based on redundant measurements [16], [17] but do not give information on the amount and origin of the calibration residual uncertainty.

Manuscript received May 1, 2013; revised September 6, 2013; accepted October 1, 2013. This work was supported in part by the Swiss National Science Foundation under Grant PMPDP2 139697 and in part by the Millimeter Wave Electronics Laboratory, ETH Zürich, Zürich, Switzerland. The Associate Editor coordinating the review process was Dr. Matteo Pastorino.

V. Teppati is with the Millimeter-Wave Electronics Group, ETH Zürich, Zürich 8092, Switzerland (e-mail: valeria.teppati@mwe.ee.ethz.ch).

A. Ferrero is with the Department of Electronics and Telecommunications, Politecnico di Torino, Torino 10129, Italy.

Color versions of one or more of the figures in this paper are available online at http://ieeexplore.ieee.org.

Digital Object Identifier 10.1109/TIM.2013.2287796

The two software tools have substantial differences in the approach and implementation, and, due to the complexity of the problem, apparently correct choices of the input quantities can lead to errors that are difficult to identify without a benchmark. Since they are the only currently available tools and have never been applied on-wafer, a careful comparison and investigation is required.

The purposes of this paper are as follows:

1) to demonstrate the applicability of these software tools in on-wafer environment;
2) to provide general guidelines for the choice of the input parameters that describe the main uncertainty contributions, i.e., vector network analyzer (VNA) noise, probe repeatability, and standard uncertainty, by an extensive comparison of the results, highlighting also the possible errors, limitations, and strong points of both approaches;
3) to present an application of these software tools to the propagation of uncertainties in a 16-term error model, showing the differences in sensitivity of the various calibration standard sequences.

This paper is structured as follows. Section II describes in details the two software tools used for the uncertainty evaluation.

Sections III compares the measurement noise, connection repeatability, and standard uncertainty contributions to the final uncertainty, providing guidelines for using them successfully in on-wafer test systems. Examples highlighting the amount of error that can arise from a poor choice of the input quantities are given.

In Section IV, a new application to a 16-term calibration model is described. Suggestions for the choice of the best standard sequence are presented. Finally, Section V draws the conclusions of this paper.

II. Available Software Tools

We consider the following applications.

1) SW1: VNA Tools II [18], provided free of charge by the Swiss Metrological Institute (METAS) and available at [19].
2) SW2: MMS4, a commercial software application recently developed by HFE [20].

SW1, implemented in C#, is based on linear uncertainty propagation algorithms developed within a C# library (also available from METAS) called Metas.UncLib [21], [22]. The library exploits automatic differentiation techniques [23] to keep track of and update the sensitivities of the parameters to the various input quantities, throughout the mathematical

operations needed to obtain the final calibrated *S*-parameters. SW2, developed in C++, implements the *S*-parameter uncertainty computation in a sophisticated and fully analytical way, described in [24].

Both software tools take into account the following contributions:

1) VNA noise;
2) cable and connection repeatability;
3) standard definition uncertainty.

In addition, SW1 considers the drift and the linearity of the VNA as uncertainty contributions.

The covariance information between *S*-parameters at different frequencies is available only with SW1, while both tools provide covariance estimates of *S*-parameters frequency by frequency.

With SW1, the uncertainty computation can be carried out only in a second step after measurements, by postprocessing all the collected data. SW2 computes and stores the data that characterizes the system and performs automatically the uncertainty evaluation each time a new measurement is triggered. The analytical approach of SW2 guarantees a substantial reduction of computational time, which is important for multiport *S*-parameter measurements.

In conclusion, the two applications use such different approaches that they can lead to very different uncertainty estimates if the input parameters are not properly chosen, as shown in the next section.

III. Uncertainty Comparison and Guidelines for the Choice of Input Quantities

All comparisons are performed on-wafer by measuring a set of calibration standard devices, verification standards, and DUTs with the two uncertainty packages and with WinCalXE software by CascadeMicrotech [25] (as additional check) in close sequence, by maintaining the probe contact constant throughout the measurements. These measurements can be thus considered equal but for the VNA noise: drift and probe repeatability do not perturb the data since measurements are performed close in time and without reconnection.

As will be shown in the following, measurement noise is not an issue, since we have verified that its contribution is typically negligible.

Experiments have been performed with an HP8510 VNA in the frequency range between 0.5 and 40 GHz, and with an HP8510-XF VNA in the frequency range between 0.5 and 110 GHz.

A. VNA Noise

The two uncertainty applications treat the measurement noise contribution in different ways. SW1 allows specification of a noise floor and a trace noise (magnitude and phase), while SW2 implements the methodology described in [24] for the calculations of high- and low-level noise.

When a suitable number of averages (or a sufficiently narrow IF bandwidth) is chosen, the VNA noise is typically very small with respect to other contributions. In a first approximation, then, the noise floor of SW1 can be set equal to the low-level noise in SW2, while the trace noise of SW1 can be set equal to the high-level noise of SW2. This leads to minimal differences between the final uncertainties obtained with the two applications.

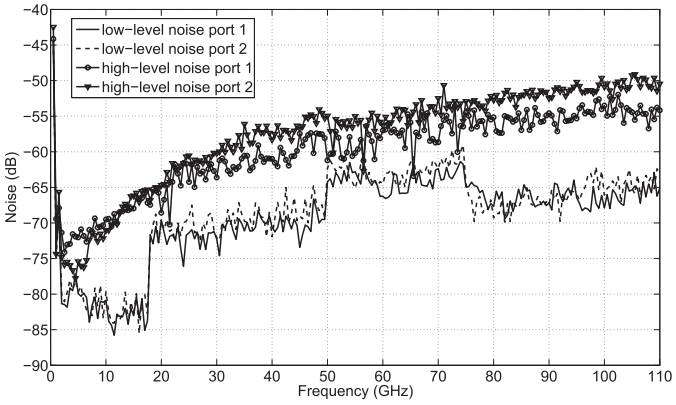

Fig. 1. High- and low-level noise contributions with the HP8510-XF VNA, with 101 average factor (data from SW2).

Since it is mainly devoted to metrological applications, SW1 takes into account also the additional contributions of linearity and drift. In the typical testing environment, linearity is not an issue as long as measurements are performed keeping the power level constant. Moreover, if the measurements are performed after a warming-up time of some hours and the VNA is calibrated periodically, also the drift is negligible. This is why in this paper these contributions to uncertainty will not be considered.

The system noise was characterized for the 40- and 110-GHz setups, with SW2. The 40-GHz system's low-level noise is always below -90 dB over the entire frequency range, while the high-level noise ranges from -70 dB at 1 GHz to -50 dB at 40 GHz. The 110-GHz system's low- and high-level noise contributions are plotted in Fig. 1. It can be clearly seen how the low-level noise depends on the band of operation, but never exceeds -60 dB, thus being negligible for on-wafer applications. The high-level noise contribution is higher, but does not appreciably affect the final uncertainty budget.

B. Connection and Cable Repeatability

The contribution to the final *S*-parameter uncertainty of the connections is particularly important on-wafer and as the frequency increases to millimeter waves. The two applications use different approaches since SW1 is optimized for coaxial measurements.

SW1 uses two different models for cable and connector repeatability [19]. Calling a_C and b_C the waves at the reference plane where the DUT or the standard is defined, and a and b the waves affected by the cable repeatability, as shown in Fig. 2, SW1 imposes the following relationships:

$$\begin{aligned} b &= C_P b_C \\ a &= \frac{1}{C_P} a_C \end{aligned} \tag{1}$$

where C_P is a transmission only term random variable with mean value equal to 1 and variance v_{C_P}.

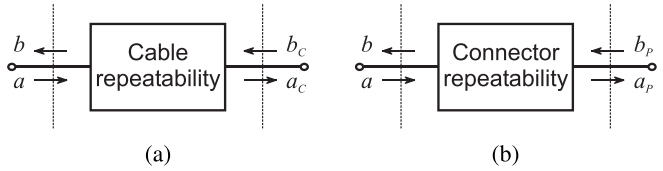

Fig. 2. Wave definitions for (a) cable and (b) connector repeatability.

The connector repeatability is treated with the following model:

$$\begin{aligned} b &= R_P a + b_P \\ a_P &= a + R_P b_P \end{aligned} \tag{2}$$

where a and b are, as before, the waves affected by the repeatability, and a_P and b_P are the waves at the reference plane where the DUT or the standard is defined. R_P is a reflection only term random variable, with mean value equal to zero and variance υ_{R_P}.

When both repeatability models are cascaded, waves a and b in (2) become, respectively, equal to a_C and b_C of (1). Thus, (2) can be rewritten as

$$\begin{aligned} b_C &= R_P(a_P - R_P b_P) + b_P \\ a_C &= a_P - R_P b_P. \end{aligned} \tag{3}$$

By neglecting the second-order terms and substituting (1) in (3), we get

$$\begin{aligned} b &\approx C_P b_P + C_P R_P a_P \\ a &\approx -\frac{R_P}{C_P} b_P + \frac{1}{C_P} a_P \end{aligned} \tag{4}$$

and finally

$$\begin{aligned} b &\approx C_P b_P + R_P a_P \\ a &\approx -R_P b_P + \frac{1}{C_P} a_P. \end{aligned} \tag{5}$$

This model for the repeatability is now formally the same as the model proposed in [24] and implemented in SW2, which takes into account cable and connector transmission and reflection repeatability terms and is defined as follows [24, (48)]:

$$\begin{aligned} b &= (1 + \delta_T) b_P + \delta_R a_P \\ a &= -\delta_R b_P + (1 - \delta_T) a_P. \end{aligned} \tag{6}$$

Here, δ_T and δ_R are two correlated random variables, with zero mean values and variances υ_R and υ_T and covariance υ_{TR}.

A comparison is still possible by neglecting the covariance and setting the same variances in both models, i.e., $\upsilon_{C_P} = \upsilon_T$ and $\upsilon_{R_P} = \upsilon_R$.

The results of a repeatability characterization performed as described in [24], with 20 contacts of an on-wafer GSG-40A-150-P (Picoprobe) probe, are shown in Fig. 3. From this figure and the next considerations, it will be evident that the υ_T contribution to the repeatability cannot be neglected for a typical on-wafer setup.

The measurement of a "thru" device was used to compare the repeatability contributions.

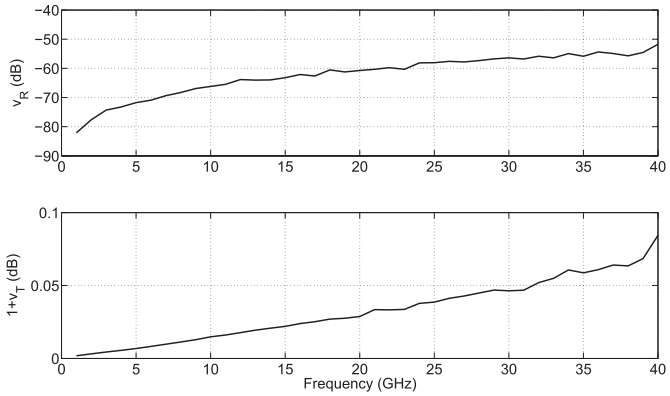

Fig. 3. Measured repeatability of an on-wafer GSG-40A-150-P (picoprobe) probe, according to the model presented in [24].

The applied calibration algorithm was the short open load reciprocal (SOLR) [26] and the same standard definitions were used in the three software applications, leading to the same nominal value of the measurement (thus confirming that the VNA noise contribution is negligible for our purposes).

Other calibration algorithms such as line reflect match (LRM) and "Thru" reflect line (TRL) were compared, but in the following we will focus on the SOLR calibration, since its greater number of required standards increases both the probe repeatability and the standard definition uncertainty contributions.

In a first experiment, since small movements of the on-wafer probes are involved, the cable effect is negligible, thus only the on-wafer probe repeatability term R_P is considered, while C_P is set to zero. As shown in Fig. 4, the uncertainties of a "thru" transmission parameter (in magnitude and phase) significantly differ if computed with SW1 and SW2. In particular, SW1 underestimates the computation of S_{12} (and S_{21}) phase uncertainty because only the connector reflection repeatability term is taken into account (with variance $\upsilon_{R_P} = \upsilon_R$). However, once the cable repeatability contribution is included (with variance $\upsilon_{C_P} = \upsilon_T$), SW1 leads to the same uncertainty levels as SW2, as is evident from Fig. 5. The small differences can be attributed to the lack of covariance information in the repeatability model of SW1.

In a typical on-wafer application, the movements of the cables are actually negligible, but when characterizing the probe repeatability as described in [24], the term υ_{C_P} cannot be neglected. Indeed, SW1 was specifically designed for coaxial measurements, but still the on-wafer repeatability can be easily modeled by adding this "dummy" cable repeatability contribution.

C. Standard Definition Uncertainty

In both software tools it is possible to import a standard definition from a file (a data-based standard), with its associated user-defined covariance matrices. In this way, both applications can avoid mistakes due, for example, to polynomial fitting, and uncertainties can be completely customized.

Concerning lumped element standard models, the two software tools use different methods to take into account

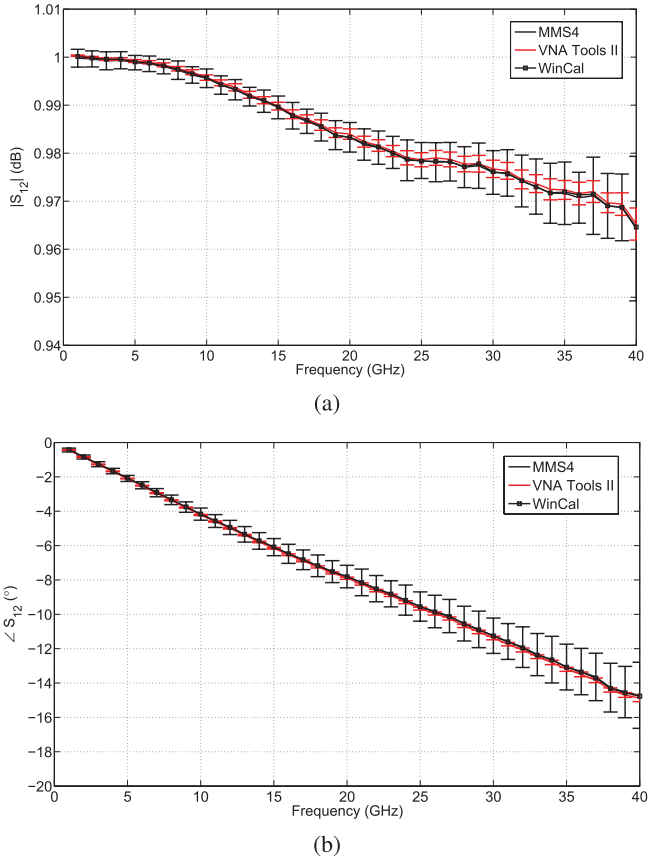

Fig. 4. Effect of repeatability uncertainty alone on the (a) magnitude and (b) phase of the transmission of a "thru" (1σ uncertainty is plotted). Measurements were calibrated with a SOLR method, using the same standard definition in all the software packages. For SW1 (VNA Tools II) the connector repeatability was set equal to SW2 (MMS4) and the cable repeatability contribution was neglected.

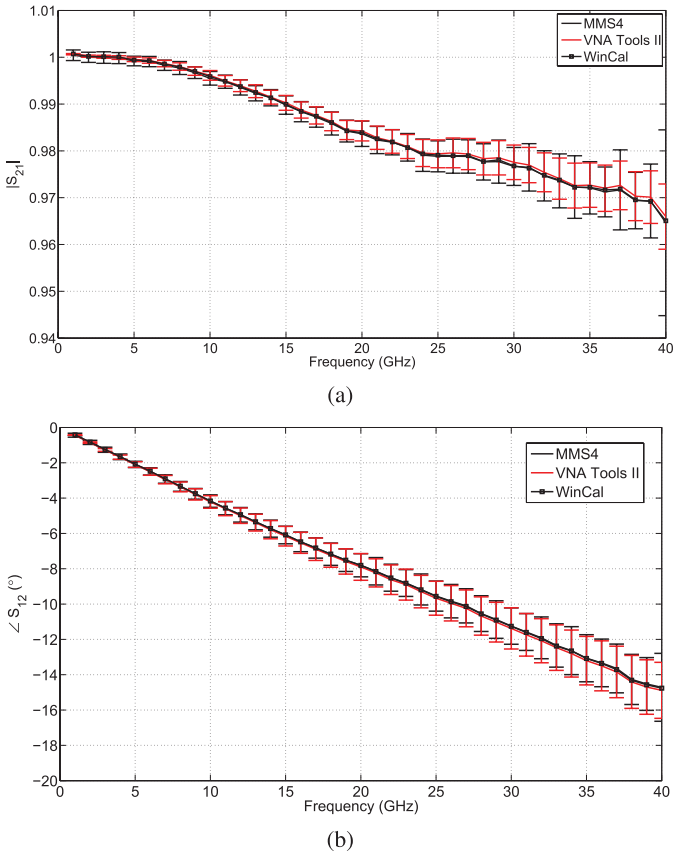

Fig. 5. Effect of repeatability uncertainty on the same "thru" measurement of Fig. 4 (1σ uncertainty is plotted). This time, SW1 (VNA Tools II) includes the cable repeatability effect, set equal to the SW2 contribution ($v_{C_P} = v_T$).

uncertainty on the standard's definition. In particular, in SW1 it is not possible to take into account the uncertainties on the "thru" and on the load definitions, while for the reflective standards (opens and shorts) it allows specification of only a "phase deviation"; for example, a phase deviation of 1° results in a (1σ) standard uncertainty of $\pm 0.5°$ on the phase and a standard uncertainty of ± 0.0087 on the magnitude, while with a phase deviation of 10°, the standard uncertainties on phase and magnitude become, respectively, $\pm 5°$ and ± 0.087.

In other words, with this uncertainty model, the real and imaginary parts of the standard uncertainty are 100% correlated.

SW2 has, instead, a more complex model for the standard uncertainty, which takes into account the following contributions [24].

1) "Thru":
   a) $u(\tau)$, uncertainty of delay line length τ;
   b) $u(Z_C)$, uncertainty of the line characteristic impedance Z_C;
   c) $u(L)$, uncertainty of losses (GΩ/s).
2) Load:
   a) $u(\tau)$;
   b) $u(Z_C)$;
   c) $u(L)$;
   d) $u(R)$, uncertainty of parasitic series resistance;
   e) $u(L_0)$, uncertainty of parasitic series inductance.
3) Reflects:
   a) $u(\tau)$;
   b) $u(Z_C)$;
   c) $u(L)$;
   d) $u(L_0),\ldots,u(L_3)$, $u(C_0),\ldots,u(C_3)$, uncertainties of parasitic inductances for shorts and capacitances for opens;
   e) $u(R_{\text{series}})$, $u(R_{\text{shunt}})$, uncertainties of parasitic resistances of shorts and opens, respectively.

A comparison has been made by applying the SOLR algorithm (more sensitive to standard definitions) to calibrate the measurements performed with both applications. For this comparison, the noise and repeatability contributions were completely neglected.

The definition of the standard uncertainties were set to keep the phase uncertainties of the reflects equal for the two applications. For example, in SW1 the short was specified to have a phase deviation of 3° at 110 GHz, which led to ± 0.027 uncertainty on magnitude and $\pm 1.5°$ on phase, while in SW2 the same standard was specified to have uncertainty $u(L_0) =$ 1.3 pH at 110 GHz, thus obtaining ± 0.0008 uncertainty on magnitude and $\pm 1.5°$ on phase.

The obtained differences are in some cases very small, as shown in Figs. 6 and 7, where the measurements of a line and

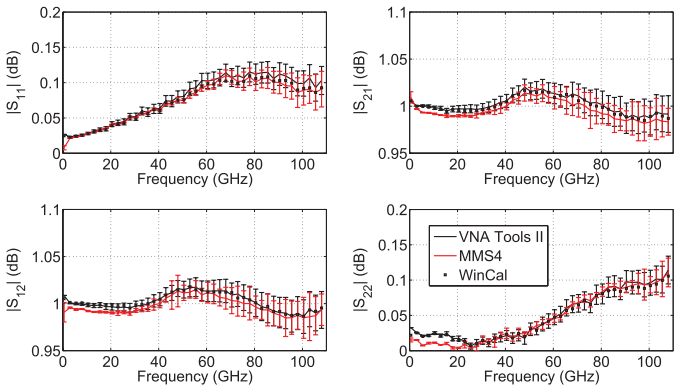

Fig. 6. Comparison of the effect of the uncertainty ($1\,\sigma$) on the standard definition on a line measurement, calibrated with a SOLR algorithm.

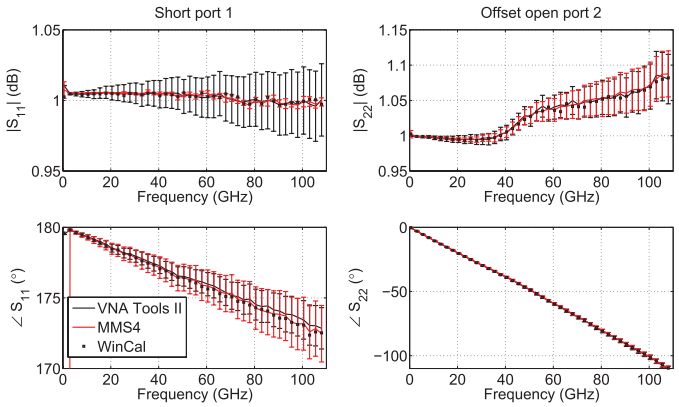

Fig. 7. Comparison of the effect of the uncertainty ($1\,\sigma$) on the standard definition on a short measurement (not used during calibration) and on an offset open measurements, calibrated with a SOLR algorithm.

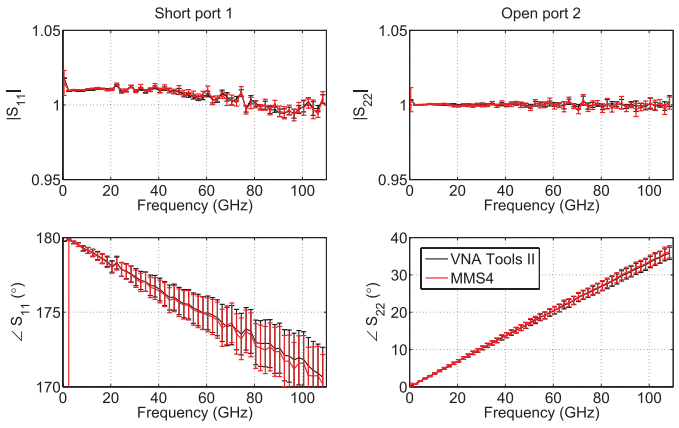

Fig. 8. Comparison of the effect of the uncertainty ($1\,\sigma$) on the standard definition on a short and on a open measurement (not used during calibration), calibrated with a SOLR algorithm, where the definitions of opens and shorts are exactly the same for both applications (loaded from file).

of two different reflective DUTs are reported. The short measurement, reported on the left of Fig. 7, highlights some discrepancies between the two software tools: the uncertainty on the short definition is transferred directly on the final measurement, thus the two applications provide different magnitude uncertainties.

TABLE I
TYPICAL PERCENTAGE OF STANDARD DEFINITION UNCERTAINTY WITH SW1 AND SW2, AT 110 GHZ, FOR ACTIVE DEVICES *S*-PARAMETERS

parameter	SW1 definition	SW2 definition
S_{11}	60-70 %	15-20 %
S_{12}	70-75 %	15-20 %
S_{21}	75-80 %	30-35 %
S_{22}	30-40 %	5-10 %

In this case, neglecting the correlation between the real and imaginary part gives a physically incorrect evaluation of the uncertainty.

To avoid these types of problems with both software tools, it is possible to load a standard definition from a file, along with its covariance matrix. When this is done, results are exactly the same. Fig. 8 reports the results for the SOLR calibration where opens and shorts were defined from files having different formats, but based on the same data. The extremely small differences (always less than 0.3%) are due to measurement noise and thus unavoidable in our comparison.

As a further example, we have considered the *S*-parameter measurements of different transistors biased in different conditions. We measured an InP heterojunction bipolar transistor with $V_{CE} = 1.2$ V and I_B ranging from 400 to 700 μA and two GaN high electron mobility transistors (HEMTs) with different sizes, biased at $V_{DS} = 5$ and 10 V, with V_{GS} ranging between -0.5 V and -3 V. Data were calibrated with the SOLR technique, using the standard uncertainty definitions of the previous example. In all cases, the results highlighted that the amount of standard definition uncertainty differs significantly when using different standard uncertainty models; in particular, SW1 always overestimates the standard uncertainty contribution for all *S*-parameters. As already pointed out, this is due to the absence of correlation between the real and imaginary part in the reflective standard uncertainty model. Table I summarizes the results obtained at 110 GHz.

D. Frequency Correlation

Frequency correlation does not affect the *S*-parameter uncertainty, but is important when different frequency points are used to compute a final output quantity [27]. Here, is a nonexhaustive list of examples:

1) extraction of a transistor (or of a diode) electrical model parameters from its *S*-parameter measurements [28]–[30];
2) power meter calibration at metrological level [31];
3) computation of the "synthetic" time-domain response of a network (i.e., time-domain reflectometry);
4) computation of time-domain waveforms in instruments/systems such as electrooptic measurement systems, high-frequency sampling oscilloscopes, large-signal network analyzers, time-domain waveform load-pull systems [27];
5) extraction of the maximum oscillation frequency (f_{MAX}) or cut-off frequency (f_T) of a transistor.

TABLE II
f_{MAX} RELATIVE UNCERTAINTY (1σ) VERSUS THE NUMBER OF POINTS FOR THE EXTRACTION, WITH AND WITHOUT COVARIANCE INFORMATION

n	$\frac{u(f_{MAX})}{f_{MAX}}$ (no covariance)	$\frac{u(f_{MAX})}{f_{MAX}}$ (with covariance)
1	4.7 %	4.7 %
3	3.8 %	4.7 %
20	1.5 %	4.8 %
40	1 %	4.9 %

In order to show the effects of frequency correlation, we focus here on the computation of the maximum oscillation frequency f_{MAX} of a transistor. In this case, a chosen gain parameter needs to be extrapolated—in the simplest case with a -20 dB/dec slope. This involves a mean operation on n points, and it is well known that, if n variables have all the same absolute uncertainty and are uncorrelated, the mean operation reduces the absolute uncertainty by a factor $1/\sqrt{n}$, while if they are perfectly correlated the mean operation does not change the absolute uncertainty.

Now, SW1 takes into account frequency correlation, typically introduced by the standard definition, while SW2 completely neglects it. As an example of how this can affect uncertainty, Table II summarizes some results obtained for a GaN HEMT having $f_{MAX} = 110$ GHz, with and without frequency correlation. When a larger number of points are included in the extrapolation, and the covariance matrices between the different frequency points are neglected, the uncertainty (1σ) drops from 4.7% to 1%. On the other hand, when correlation is considered, the uncertainty shows a small increase.

IV. UNCERTAINTY PROPAGATION FOR THE FULL-LEAKY TWO-PORT ERROR MODEL

Along with SW1, a specific MATLAB library (Metas. UncLib) is also available to create and propagate uncertainties [22].

A useful application of the combination of both software tools and the Metas.UncLib is the possibility to have information on the uncertainty of calibration algorithms and error models not implemented in the described tools. An interesting example consists in calibrating a two-port VNA affected by leakage between ports with a 16-term error model and computing its uncertainty.

According to [32], up to 36 different combinations of 5 two-port standards exist to calibrate a two-port leaky VNA. Other combinations are possible [33] but are redundant, meaning that they are obtained using the same standards in a different order. The two-port standards that avoid changing the probe separation and that are typically available on commercial calibration substrates are the following:

1) "thru" (T);
2) short at port 1—short at port 2 (SS);
3) matched load at port 1—matched load at port 2 (MM);
4) open at port 1—open at port 2 (OO);
5) short at port 1—open at port 2 (SO) or vice versa (OS);
6) matched load at port 1—open at port 2 (MO) or vice versa (OM).

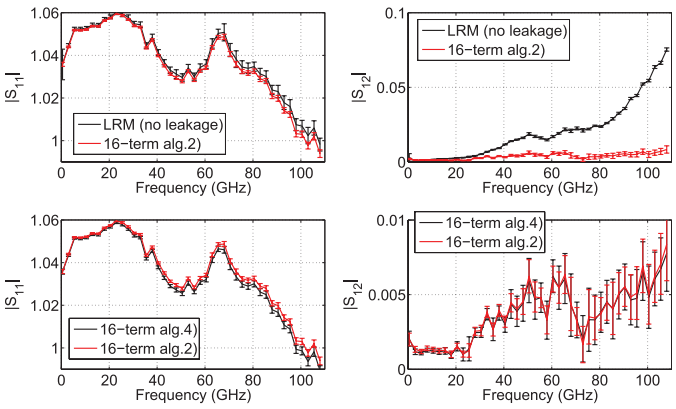

Fig. 9. Comparison of an LRM calibration and the implemented 16-term calibrations. Two shorts not used during calibration are corrected with LRM of SW2 and leaky alg. 2) and 4). 1σ uncertainty is plotted.

The reason for avoiding changes of probe separation during calibration and measurements is that it heavily affects the amount of leakage between the probes, thus invalidating the calibration results.

This cuts down the nonsingular and nonredundant combinations described in [32] as follows:

1) T, MM, SS, OO, SO (Algorithm 1);
2) T, MM, SS, SO, OS (Algorithm 2);
3) T, MM, SS, SO, MO (Algorithm 3);
4) T, MM, SS, OM, MO (Algorithm 4).

Some experiments have been performed to analyze the uncertainty of these four calibration sequences.

Attention was paid to the standard definition. In particular, the delay of the "thru" standard was computed by applying the SOLR algorithm and resulted in 0.95 ps, while the reflect standard definitions were taken to be equal to those obtained with the nonleaky LRM algorithm. This is acceptable, as the leakage below -20 dB is negligible for high reflection coefficient measurements and this is the case for our setup up to 110 GHz.

Some of the results of the various comparisons are shown in Fig. 9, where the measurements of two shorts not used during calibration are plotted. It is evident how the traditional 8-term LRM algorithm fails to correct the leakage between ports (S_{21} and S_{12}). The uncertainty on probe positioning, noise, and standards cannot take into account this systematic error, which is however corrected by the 16-term model.

Moreover, the results of the comparison of the four 16-term algorithms evidenced that, on average, Algorithms 3 and 4 showed a slightly higher uncertainty than Algorithms 1 and 2, as can be seen in Fig. 9, where the uncertainty of Algorithms 2 and 4 can be directly compared. An explanation for this can be found in Fig. 10, which shows the condition number of the four calibration systems as a function of frequency and confirms that Algorithms 1 and 2 are better conditioned than Algorithms 3 and 4.

Finally, Fig. 11 shows an example where the 16-term calibration is applied to a transistor. The device is a GaN

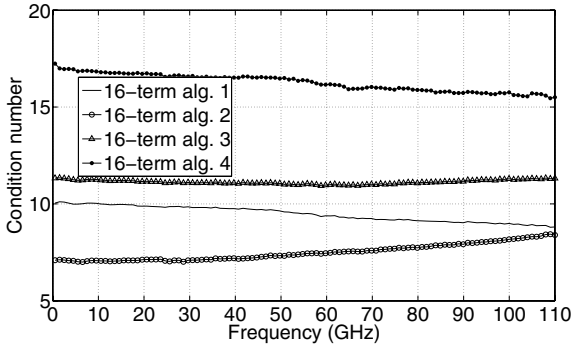

Fig. 10. Condition number of the systems solved (by matrix inversion) during calibrations 1)–4).

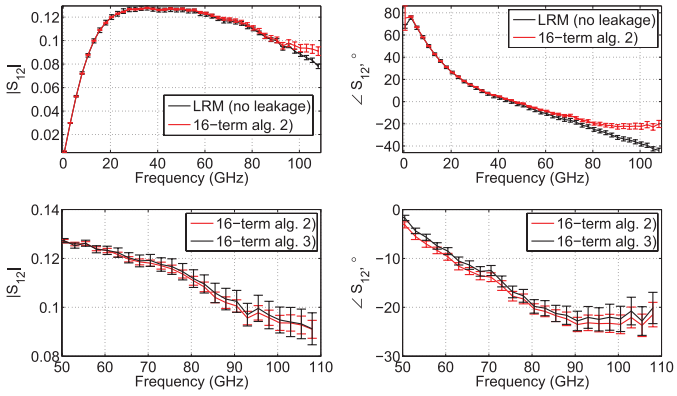

Fig. 11. GaN HEMT, biased at $V_{DS} = 5$ V and $V_{GS} = -0.75$ V, calibrated with a nonleaky LRM and two different 16-term algorithms. 1σ uncertainty is plotted.

HEMT biased at $V_{DS} = 5$ and $V_{GS} = -0.75$ V. The main difference with respect to a nonleaky calibration is typically seen in the S_{12} parameter, in both magnitude and phase. Such a difference can have a nonnegligible effect when computing the f_{MAX} of the transistor extrapolating the unilateral gain U. This is clear by looking at its definition

$$\mathrm{U} = \frac{1}{2} \frac{\left| \frac{S_{21}}{S_{12}} - 1 \right|^2}{k \left| \frac{S_{21}}{S_{12}} \right| - \mathrm{Re}\left(\frac{S_{21}}{S_{12}} \right)} \tag{7}$$

where k is the stability factor given by

$$k = \frac{1 - |S_{11}|^2 - |S_{22}|^2 + |\Delta|^2}{2|S_{12}S_{21}|} \tag{8}$$

and

$$\Delta = S_{11}S_{22} - S_{12}S_{21}. \tag{9}$$

The typically small S_{12} parameter appears at the denominator of (7), thus making U extremely sensitive to its variations.

In the specific case, $f_{MAX} = 130$ GHz for the nonleaky calibration and 138 GHz with the 16-term one, corresponding to an error of more than 6%. Also in this case, the direct comparison of the uncertainty of Algorithms 2 and 3 shows that the former brings a lower uncertainty. The reason lies again in the condition number of the calibration system, as shown in Fig. 10.

V. Conclusion

In this paper, two recently available software tools for *S*-parameters uncertainty computation have been carefully compared. Although profoundly different in the implementation, it has been possible to obtain compatible results, thus proving and validating their reliability.

The comparison has shown that the input quantities for the final computation of the uncertainty, i.e., VNA noise, probe repeatability, and standard uncertainty, must be properly chosen, and some hints on how to perform the choice were given. In particular, VNA noise is typically negligible on-wafer; concerning repeatability, the difference in the two approaches suggests that the cable repeatability contribution of SW1 must actually be taken into account on wafer; for the standard definition, the approach of SW1 for shorts and opens has some limitations due to the absence of real and imaginary part correlation. Several examples on how these contributions can affect final measurements were given, in addition to an example of the effect of frequency correlation on the extraction of parameters from n measurement points.

We finally remark that the possible applications of these tools, at both the metrological level and in the testing environment, are practically limitless. Being able to quantify uncertainties and perform sensitivity studies (such as the leaky-calibration uncertainty evaluation presented here) can be crucial when calibration standards have higher uncertainties, for example, when they are designed on the same substrate of an active DUT or of an monolithic microwave integrated circuit.

Acknowledgment

The authors would like to thank the developers of the software tools used in this paper, M. Garelli (HFE) and M. Wollensack (METAS), for their help and support.

References

[1] J. P. Hoffmann, P. Leuchtman, A. Kretz, J. Rüfenacht, and R. Vahldieck, "Characterization of coaxial adapters for S-parameter measurements," in *Proc. 38th Eur. Microw. Conf.*, Amsterdam, The Netherlands, Oct. 2008, pp. 313–316.

[2] D. F. Williams, "500 GHz–750 GHz rectangular-waveguide vector-network-analyzer calibrations," *IEEE Trans. Terahertz Sci. Technol.*, vol. 1, no. 2, pp. 364–377, Nov. 2011.

[3] K. Wong, "Traceability of vector network analyzer measurements," in *Proc. 72nd ARFTG Microw. Meas. Conf.*, Portland, OR, USA, Dec. 2008, pp. 157–167.

[4] N. Ridler, R. Clarke, M. Salter, and A. Wilson, "Traceability to national standards for S-parameter measurements in waveguide at frequencies from 220 GHz to 330 GHz," in *Proc. Microw. Meas. Symp.*, Tempe, AZ, USA, Dec. 2011, pp. 1–6.

[5] M. Horibe and N. M. Ridler, "Comparison between NPL and NMIJ of diameter and scattering parameter measurements of precision 1.85 mm coaxial air lines," *IEEE Trans. Instrum. Meas.*, vol. 60, no. 7, pp. 2327–2334, Jul. 2011.

[6] M. Horibe and R. Kishikawa, "Traceability to national standards for S-parameter measurements in waveguide at 1.1 THz," in *Proc. CPEM*, Washington, DC, USA, Jul. 2012, pp. 254–255.

[7] J. Martens, "LRM: A quantitative look at reference impedance contradictions and other uncertainty impacts," in *Proc. 69th ARFTG Microw. Meas. Conf.*, Honolulu, HI, USA, Jun. 2007, pp. 1–7.

[8] U. Stumper and T. Schrader, "Influence of different configurations of nonideal calibration standards on vector network analyzer performance," *IEEE Trans. Instrum. Meas.*, vol. 61, no. 7, pp. 2034–2041, Jul. 2012.

[9] A. M. E. Safwat and L. Hayden, "Sensitivity analysis of calibration standards for SOLT and LRRM," in *Proc. 58th ARFTG Microw. Meas. Conf.*, San Diego, CA, USA, Nov. 2001, pp. 1–10.

[10] A. Rumiantsev, P. Corson, S. Sweeney, and U. Arz, "Applying the calibration comparison technique for verification of transmission line standards on silicon up to 110 GHz," in *Proc. 73rd ARFTG Microw. Meas. Conf.*, Boston, MA, USA, Jun. 2009, pp. 1–6.

[11] W. V. Moer, "Development of new measuring and modeling techniques for RFICS and their nonlinear behavior," Dept. ELEC, Faculteit Toegepaste Wetenschappen, Vrije Universiteit Brussel, Brussels, Belgium, 2001.

[12] J. Leinhos and U. Arz, "Establishing uncertainties for on-wafer S-parameter measurements," in *Proc. GeMIC*, Harburg, Germany, Mar. 2008, pp. 439–441.

[13] J. Hoffmann, P. Leuchtmann, J. Schaub, and R. Vahldieck, "Computing uncertainties of S-parameters by means of Monte Carlo simulation," in *Proc. 69th ARFTG Microw. Meas. Conf.*, Honolulu, HI, USA, Jun. 2007, pp. 1–7.

[14] H. Hui, L. Xinmeng, and L. Xin, "Monte Carlo analysis of measurement uncertainties for on-wafer short-open-load-reciprocal calibrations," in *Proc. Asia-Pacific Microw. Conf.*, Melbourne, Australia, Dec. 2011, pp. 1778–1781.

[15] J. Leinhos and U. Arz, "Monte-Carlo analysis of measurement uncertainties for on-wafer thru-reflect-line calibrations," in *IEEE MTT-S Int. Microw. Symp. Dig.*, Atlanta, GA, USA, Jun. 2008, pp. 33–36.

[16] A. Arsenovic, L. Chen, M. F. Bauwens, H. Li, N. S. Barker, and I. R. M. Weikle, "An experimental technique for calibration uncertainty analysis," *IEEE Trans. Microw. Theory Tech.*, vol. 61, no. 1, pp. 263–269, Jan. 2013.

[17] D. F. Williams, J. C. M. Wang, and U. Arz, "An optimal vector-network-analyzer calibration algorithm," *IEEE Trans. Microw. Theory Tech.*, vol. 51, no. 12, pp. 2391–2401, Dec. 2003.

[18] M. Wollensack, J. Hoffmann, J. Ruefenacht, and M. Zeier, "VNA tools II: S-parameter uncertainty calculation," in *Proc. 79th ARFTG Conf.*, Montreal, QC, Canada, Jun. 2012, pp. 1–5.

[19] M. Wollensack and J. Hoffmann. (2012, Apr.). *METAS VNA Tools II—Math Reference* [Online]. Available: http://www.metas.ch/vnatools.

[20] HFE Sagl, San Vittore, Switzerland. (2013, Oct. 31). *Multiport S-Parameters Software—MMS4* [Online]. Available: http://www.hfemicro.com.

[21] M. Zeier, J. Hoffmann, and M. Wollensack, "Metas.UncLib—A measurement uncertainty calculator for advanced problems," *Metrologia*, vol. 49, no. 6, pp. 809–815, 2012.

[22] M. Wollensack and M. Zeier. (2011, Nov.). *Metas.UncLib—An Advanced Measurement Uncertainty Calculator* [Online]. Available: http://www.metas.ch/unclib.

[23] B. D. Hall, "Calculating measurement uncertainty using automatic differentiation," *Meas. Sci. Technol.*, vol. 13, no. 4, pp. 421–427, 2002.

[24] A. Ferrero and M. Garelli, "A unified theory for *S*-parameter uncertainty evaluation," *IEEE Trans. Microw. Theory Tech.*, vol. 60, no. 12, pp. 3844–3855, Dec. 2012.

[25] (2013, Oct. 31). *CascadeMicrotech WinCalXE Software* [Online]. Available: http://www.cmicro.com/products/probes/wincal-xe.

[26] A. Ferrero and U. Pisani, "Two-port network analyzer calibration using an unknown 'thru'," *IEEE Microw. Guided Wave Lett.*, vol. 2, no. 12, pp. 505–507, Dec. 1992.

[27] A. Lewandowski, D. Williams, P. Hale, C. M. Wang, and A. Dienstfrey, "Covariance-matrix-based vector-network-analyzer uncertainty analysis for time-and frequency-domain measurements," *IEEE Trans. Microw. Theory Tech.*, vol. 58, no. 7, pp. 1877–1866, Jul. 2010.

[28] C. Fager, P. Linner, and J. Pedro, "Uncertainty estimation and optimal extraction of intrinsic FET small signal model parameters," in *IEEE MTT-S Int. Microw. Symp. Dig.*, Seattle, WA, USA, Jun. 2002, pp. 729–732.

[29] S. M. Masood, T. K. Johansen, J. Vidkjaer, and V. Krozer, "Uncertainty estimation in SiGe HBT small-signal modeling," in *Proc. Eur. Gallium Arsenide Other Semicond. Appl. Symp.*, Paris, France, Oct. 2005, pp. 393–396.

[30] J. Martens, "Parameter extraction from 110+ GHz S-parameter measurements: A heuristic analysis of sensitivity and uncertainty propagation," in *Proc. IEEE Int. Conf. Microw., Commun., Antennas Electron. Syst.*, Tel Aviv, Israel, Nov. 2011, pp. 1–4.

[31] T. Ling, L. Maoliu, and Z. Yichi, "Covariance-matrix-based uncertainty propagation analysis for complex-valued quantities throughout VNA S-parameter measurements and power-meter calibration," in *Proc. CPEM*, Washington, DC, USA, Jul. 2012, pp. 1–7.

[32] K. Silvonen, "LRM 16-A self calibration procedure for a leaky network analyzer," *IEEE Trans. Microw. Theory Tech.*, vol. 45, no. 7, pp. 1041–1049, Jul. 1997.

[33] K. Silvonen. (1998, Jul.). *New Five-Standard Calibration Procedures for Network Analyzers and Wafer Probes* [Online]. Available: http://users.tkk.fi/ksilvone/Calibration/ct-19.pdf.

Valeria Teppati (S'01–M'03–SM'12) was born in Torino, Italy. She received the Laurea degree (*summa cum laude*) in electronic engineering and the Ph.D. degree in electronic instrumentation from Politecnico di Torino, Torino, in 1999 and 2003, respectively.

She has been with the Department of Electronics, Politecnico di Torino, as an Assistant Professor, since 2003. From December 2010 to March 2011, she has been a Visiting Professor with the Millimeter-Wave Electronics Group, Eidgenoessische Technische Hochschule, Zurich, Switzerland. Since May 2012, she has been with the same group as a Researcher, with a grant funded by the Swiss National Science Foundation. Her current research interests include microwave devices design, linear and nonlinear measurement design and automation, load-pull, differential load-pull, multiport vector network analyzers, and their calibration and uncertainty.

Andrea Ferrero (S'87–M'92–F'11) was born in Novara, Italy, on November 7, 1962. He received the Electronic Engineering and Ph.D. degrees in electronics from Politecnico di Torino, Turin, Italy, in 1987 and 1992, respectively.

He joined Aeritalia Company, Turin, Italy, in 1988, as a Microwave Consultant. In 1991, he was with the Microwave Technology Division, Hewlett-Packard, Santa Rosa, CA, USA, as a Summer Student. In 1995, he was with the Department of Electrical Engineering, Ecole Polytechnique de Montreal, Montreal, QC, Canada, as a Guest Researcher. In 1998 and 2006, he became an Associate Professor and a Full Professor of electronic measurements with the Dipartimento di Elettronica, Politecnico di Torino. His current research interests include microwave measurement techniques, calibration, and modeling.

Prof. Ferrero was an IEEE Microwave Theory and Techniques Society Distinguished Microwave Lecturer from 2010 to 2012. He was a recipient of the 2006 ARFTG Technology Award for the development and implementation of VNA calibration algorithms and nonlinear measurement techniques.